

Spin-orbit effects in the ${}^8\text{Li}+{}^{58}\text{Ni}$ elastic scattering

O C B Santos¹, R Lichtenthäler¹, K C C Pires¹, A M Moro²,
U Umbelino¹, E O N Zevallos¹, M Assunção³, S Appannababu¹,
J Alcántara-Núñez¹, A L de Lara¹, V Scarduelli¹, V Guimarães¹,
A Lépine-Szily¹, A. S. Serra¹, R Linares⁴, V A B Zagatto⁴,
P N de Faria⁴, V Morcelle⁵, M C Morais⁴, A Barioni³, J M B Shorto⁶

¹Instituto de Física, Universidade de São Paulo, São Paulo, Brazil

²Departamento de Física Atómica, Molecular y Nuclear, Universidad de Sevilla, Spain

³Universidade Federal de São Paulo, SP, Brazil

⁴Universidade Federal Fluminense, RJ, Brazil

⁵Universidade Federal Rural do Rio de Janeiro, Seropédica - RJ, Brazil

⁶IPEN, Comissão Nacional de Energia Nuclear, São Paulo, Brazil

E-mail: osvaldo.santos@usp.br

Abstract. In this work we present an elastic scattering angular distribution for the ${}^8\text{Li}+{}^{58}\text{Ni}$ system measured at $E_{\text{lab}} = 26.1$ MeV. The ${}^8\text{Li}$ beam was produced in the Radioactive Ion Beams in Brasil (RIBRAS) facility using the ${}^7\text{Li}$ primary beam delivered by the 8-UD Pelletron accelerator. The angular distribution covers the angular range from 20 to 85 degrees in the center of mass frame. The data have been analysed by optical model and coupled channels calculations, including couplings to low-lying states in ${}^8\text{Li}$ and the spin-orbit interaction. Our results indicate that the inclusion of the spin-orbit interaction in the calculations is important to describe the data at backward angles.

1. Introduction.

A large research field was opened with the possibility of producing secondary beams of nuclei out of the stability valley. Several facilities became operational all over the world making this field one of the most active in the low energy nuclear physics domain [1–5]. In particular, in the region of light nuclei there are several interesting phenomena to be explored [6–8]. Light nuclei, in general, present cluster structure with low breakup energies for certain configurations. ${}^6,{}^7\text{Li}$ and ${}^9\text{Be}$ are examples of stable weakly bound light nuclei with breakup energies of $E_{\text{bu}}=1.47$ MeV, 2.46 MeV and 1.67 MeV, for $\alpha + d$, $\alpha + t$ and $\alpha + \alpha + n$ configurations respectively. As one goes always of the valley of stability, there are radioactive species, with relatively long half-lives (≈ 800 ms), and they have even lower breakup energies. Exotic structures such as neutron halos can be found for instance in ${}^6\text{He}$ ($\alpha + n + n$; $E_{\text{bu}}=0.975$ MeV) and ${}^{11}\text{Li}$ (${}^9\text{Li} + n + n$; $E_{\text{bu}}=0.37$ MeV) among others.

Although ${}^8\text{Li}$ (${}^7\text{Li} + n$; $E_{\text{bu}}=2.0$ MeV) is not considered an exotic nuclei, its possible importance to astrophysics has attracted some interest in the investigation of its structure. The synthesis of heavy elements in stars has to overcome the $A = 5$ and 8 mass gaps for which there are no stable elements. For $A = 8$, there are only two bound nuclei, ${}^8\text{Li}$ and ${}^8\text{B}$. They are mirror nuclei and have half-lives of 840 ms and 770 ms respectively, long enough to possibly affect the nucleosynthesis in stars and in the primordial Universe [9–12]. For this reason, studies involving



$A = 8$ nuclei are welcome since they can provide information of the interacting potential which is an important ingredient in calculations of cross sections involving these nuclei [13].

Here, we present an angular distribution of the $^8\text{Li} + ^{58}\text{Ni}$ elastic scattering at 26.1 MeV, which corresponds to an energy twice the Coulomb barrier for this system $V_b = 13.1$ MeV [14, 15]. Analyses with optical model(OM) and coupled channels(CC) calculations were performed using a double folding Sao Paulo potential (SPP) [16] and an important contribution of the spin-orbit interaction was identified.

2. Experimental Setup.

The 28 MeV ^7Li primary beam was delivered by the 8-UD Pelletron accelerator with an intensity between 200 and 300 enA. The ^8Li secondary radioactive ion beam was produced by the RIBRAS system using the one neutron transfer reaction $^9\text{Be}(^7\text{Li}, ^8\text{Li})$. The ^8Li beam was selected and focused by the first solenoid in the central scattering chamber. The intensity of the secondary beam was around 2×10^5 pps (per 250 enA of primary beam) in the scattering chamber. To compensate for the relatively low intensity of the radioactive ion beam, thick targets (in order of mg/cm^2) and large detection solid angles ≈ 20 msr are usually applied. The thickness of the ^{58}Ni and ^{197}Au targets were of $2.1 \text{ mg}/\text{cm}^2$ and $4.6 \text{ mg}/\text{cm}^2$, respectively. The Gold target was used to normalize the data and to obtain the absolute cross sections, assuming the $^8\text{Li} + ^{197}\text{Au}$ scattering as pure Rutherford, which is valid in the energy range of the present experiment.

The detection system consists of four ΔE -E telescopes formed by silicon surface barrier detectors of $\Delta E = 25 \text{ } \mu\text{m}$ and $E = 1000 \text{ } \mu\text{m}$ thickness.

A typical E- ΔE spectrum at $\theta_{\text{lab}} = 26^\circ$ with Gold target is presented in figure 1. We identify the ^8Li peak as well as the contaminants of the secondary beam. The contaminants are alphas, protons, deuterium, tritium and other particles such as the ^9Be , recoiling from the primary target, and ^7Li from the primary beam. A ^6He peak was identified as coming from the $^9\text{Be}(^7\text{Li}, ^6\text{He})$ reaction in the primary target.

Four $^8\text{Li} + ^{58}\text{Ni}$ angular distributions at 23.9 MeV, 26.1 MeV, 28.7 MeV, and 30.0 MeV laboratory energies were measured. Figure 2 presents the $^8\text{Li} + ^{58}\text{Ni}$ distribution at 26.1 MeV.

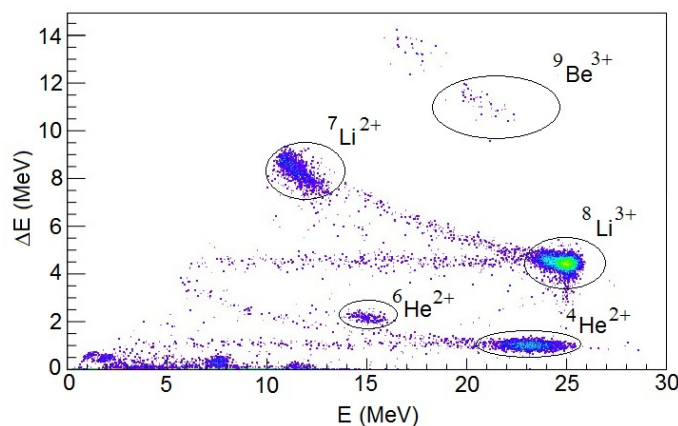


Figure 1. Typical bi-dimensional spectra obtained for $^8\text{Li} + ^{197}\text{Au}$ system at $\theta_{\text{lab}} = 26^\circ$.

3. Monte Carlo simulation.

Due to the large detection solid angles and the intrinsic angular divergence of the RIBRAS beam, it is necessary to make a correction in the nominal detection angles. This was performed using a Monte Carlo simulation code (*RIBRAS*) [17]. The simulation generates aleatory events inside

the beam spot and in the detector, tracing the ray between them and obtaining the scattering angle distribution of the events. It takes into account the angular divergence of the secondary beam, angular straggling and the geometry of the slits of the detectors. A folding between the Rutherford cross section and the angle distribution is performed to calculate the average detection angle. Cross sections different from Rutherford can be used as well. As the elastic cross section drops down quickly with angle, this correction causes a shift of the average angle to the forward direction, being more important at forward angles. An example of the corrections is shown in figure 2.

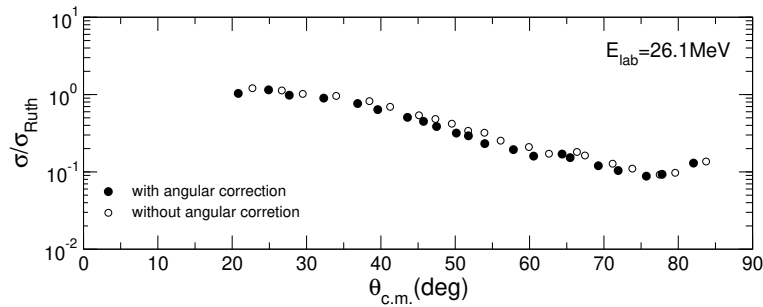


Figure 2. The ${}^8\text{Li}+{}^{58}\text{Ni}$ angular distribution with (black points) and without (white points) angular correction performed using the (*RIBRAS*) simulation.

4. Analysis and Results.

In figure 3 we present the ${}^8\text{Li} + {}^{58}\text{Ni}$ angular distribution compared with four different calculations. The blue line is an Optical Model (OM) calculation using the SPP with $N_r=1$ and $N_i=0.78$. Usually the angular distributions for exotic projectiles such as ${}^6\text{He}$ exhibit more absorption than optical model calculation with SPP and the calculations usually overestimate the experimental data at backward angles. Here, the results show the opposite, SPP calculation underestimates the experimental cross sections. This motivated us to consider different effects that could be causing this enhancement with respect to the SPP calculations. One possibility is the effect of the coupling to the first low lying ${}^8\text{Li}$ excited states on the elastic distribution. To estimate this effect we performed Coupled Channels (CC) calculations using the FRESKO program [18], including the coupling to the first 1^+ (980 keV), second 3^+ (2.26 MeV) and third 1^+ (3.21 MeV) excited states of ${}^8\text{Li}$. Only nuclear excitation was considered with a deformation length of $\delta_2=1.75$ fm [19]. The results of the CC calculations are shown as the green line in figure 3 which is a little above the OM calculation (blue line), but not sufficient to explain the data.

Another effect that could contribute to the enhancement of the cross sections comes from the fact that our energy resolution is not sufficient to separate the first excited state of ${}^8\text{Li}$ (980 KeV) from its ground-state. In this case a contamination from the inelastic excitation would be present in the elastic peak (quasi-elastic scattering) causing an enhancement of the cross section. The pink line in figure 3 corresponds to the sum of the inelastic and elastic cross section, obtained from the CC calculation. We see that there is a small effect but not sufficient to explain all the observed enhancement.

Finally, we considered the effect of the spin of the projectile in the calculation. The ${}^{6,7,8}\text{Li}$ isotope chain has, respectively, ground state spins of 1^+ , $3/2^-$ and 2^+ , ${}^8\text{Li}$ being the larger. Then we included the effect of the spin-orbit interaction (S.O.) in the OM calculations. The red line corresponds to the results of the calculations where the spin-orbit term was included. The form

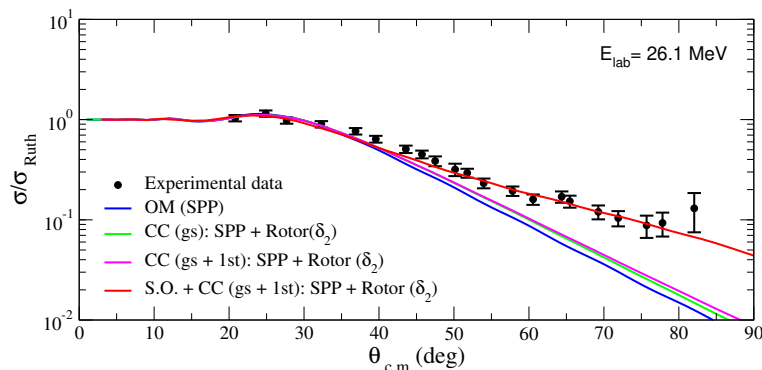


Figure 3. Angular distribution for $^8\text{Li}+^{58}\text{Ni}$ system measured at $E_{\text{lab}}=26.1$ MeV compared to calculations, as described in the text.

factor of the spin-orbit term was taken as the derivative of an Woods-Saxon, whose parameters are $V_{0s}=1.96$ MeV, $r_{0s}=1.25$ fm and $a_{0s}=0.65$ fm. The calculation were performed using the FRESKO code and V_{0s} was varied to best reproduce the data. The result is surprising and shows that the effect of spin-orbit interaction explains the data with reasonable S.O. parameters. We also performed calculations for $^6,^7\text{Li}$ data but the spin-orbit interaction seems not to be as important as in the ^8Li case.

5. Conclusions

An elastic scattering angular distribution for the $^8\text{Li}+^{58}\text{Ni}$ system is presented. The experimental cross sections at backward angles show a considerable enhancement when compared to Optical Model calculations using the Sao Paulo Potential. Coupled channels calculations were performed to investigate the effect of the projectile excitation in the angular distribution. The results show that the projectile quasi-elastic excitation gives little effect in the backward angular distribution, not sufficient to explain the observed enhancement. The inclusion of the spin-orbit interaction in the calculations can account for the observed enhancement.

6. Acknowledgment

The authors would like to thanks the Coordenação de Aperfeiçoamento de Pessoal de Nível Superior (CAPES) and Fundação de Amparo à Pesquisa do Estado de São Paulo (FAPESP) proc. 2013/22100-7 and 2016/17612-7 for financial support.

References

- [1] Lichtenthäler R, Lépine-Szily A and Guimarães V 2005 *Eur. Phys. J. A* **25** 1733
- [2] Lépine-Szily A, Lichtenthäler R and Guimarães V 2014 *Eur. Phys. J. A* **50** 128
- [3] Lépine-Szily A, Lichtenthäler R and RIBRAS collaboration 2007 *Nucl. Phys. A* **787** 94c
- [4] Lichtenthäler R, Alvarez M A G, Lépine-Szily A, Appannababu S, Pires K C C, Da Silva U U, Scarduelli V, Condori R P and Deshmukh N 2016 *Few-Body Systems* **57**(3) 157163
- [5] Blumenfeld Y, Nilsson T and Van Duppen P 2013 *Phys. Scr.* **T152** 014023
- [6] Pires K C C *et al* 2014 *Phys. Rev. C* **90** 027605
- [7] Morcelle V *et al* 2014 *Phys. Rev. C* **89** 044611
- [8] Kolata J J, Guimarães V and Aguilera E F 2016 *Eur. Phys. J. A* **52** 123
- [9] Claus E R and William S R 1988 *Cauldrons in the Cosmos* University of Chicago Press
- [10] Camargo O *et al* 2007 *Phys. Rev. C* **75** 054602
- [11] Mendes Jr D R *et al* 2012 *Phys. Rev. C* **86** 064321
- [12] Leistenschneider E *et al* 2018 *Phys. Rev. C* **98** 064601
- [13] Morcelle V *et al* 2017 *Phys. Rev. C* **95** 014615

- [14] Freitas A S, Marques L, Zhang X X, Luzio M A, Guillaumon P, Pampa-Condori R and Lichtenthäler R 2016 *Braz. J. Phys.* **46** 120128
- [15] Pires K C C, Appannababu S, Lichtenthäler R and Santos O C B 2018 *Phys. Rev. C* **98** 014614
- [16] Chamon L C, Carlson B V, Gasques L R, Pereira D, De Conti C, Alvarez M A G, Hussein M S, Cândido Ribeiro M A, Rossi Jr E S and Silva C P 2002 *Phys. Rev. C* **66** 014610
- [17] Lichtenthäler R *Ribras code Not Published*
- [18] Thompson I J 1988 *Computer Physics Reports* **7**(4) 167212
- [19] Tengborn E *et al* 2011 *Phys. Rev. C* **84** 064616